Available online at www.sciencedirect.com
SCIENCE DIRECT®
International Journal of Heat and Fluid Flow 24 (2003) 491–499
International Journal of HEAT AND FLUID FLOW
www.elsevier.com/locate/ijhff

Effect of Weissenberg number on the flow structure: DNS study of drag-reducing flow with surfactant additives

Bo Yu [a,b], Yasuo Kawaguchi [a,*]

[a] Turbomachinery Research Group, Institute for Energy Utilization, National Institute of Advanced Industrial Science and Technology, 1-2 Namiki, Tsukuba, Ibaraki 305-8564, Japan
[b] Center for Smart Control of Turbulence, National Maritime Research Institute, Japan, 6-38-1 Shinkawa, Mitaka, Tokyo 181-0004, Japan

Received 6 November 2002; accepted 14 March 2003

Abstract

A second-order finite difference scheme was employed for the DNS study of drag-reducing flow with surfactant additives. We focus on the effect of Weissenberg number (nondimensional relaxation time) on the flow structures. The instantaneous flow structures and stress distribution at different elasticities are compared. The effects of Weissenberg number on turbulence statistics such as turbulence intensities, Reynolds shear stress and two-point correlation coefficients are also presented.

Keywords: Channel flow; DNS; Drag-reduction; Giesekus model; MINMOD scheme; Surfactant solution

1. Introduction

It is well known that a small amount of chemicals such as water-soluble polymers or surfactants dramatically suppresses turbulence when they are added to liquid flow at large Reynolds number (Toms, 1948). In the last two decades, the application of surfactants to heat transportation systems such as district heating and cooling systems has attracted much interest among researchers. It has been revealed that 70% of the pumping power used to drive hot water in primary pipelines or district heating systems was saved by adding only a few hundred ppm of surfactant into the circulating water. The technological achievement requires a new design strategy for pipeline networks and heat exchangers to handle the drag reducing liquid flow. In the case of a Newtonian fluid such as water or air, the knowledge for designing fluid systems has been accumulated and the accuracy of numerical prediction is sufficient. On the other hand, the design system for surfactant solutions is not mature because drag-reducing flow phenomena are much more complicated than for Newtonian flow, for example, the friction factor for a surfactant solution depends not only on Reynolds number but also pipe diameter. In order to provide a design strategy for heat transportation systems using surfactant additives, we are now carrying out both experimental and numerical studies for surfactant solutions (Li et al., 2001; Yu and Kawaguchi, 2002).

This paper reports some results of our direct numerical simulations for surfactant solutions. The adoption of an appropriate model is the key for simulating drag-reducing flow by additives. We have found that Giesekus model can well describe the measured apparent shear viscosity and extensional viscosity of the surfactant solution. Therefore we assume that the surfactant solution is a Giesekus fluid. Some direct numerical simulations have been done for drag-reducing polymer solutions, and extensional viscosity models were employed for simulating the solutions (Orlandi, 1995; DenToonder et al., 1997). Those simulation results qualitatively agree with most of the experimental observations. However, the inelastic characteristic of the extensional models makes it impossible to examine the onset phenomenon. Recently, viscoelastic models (FENE-P model and Giesekus model) were employed and a criterion for the onset of drag-reduction was proposed (Sureshkumar et al., 1997; Dimitropoulos et al., 1998). The FENE-P model was shown to be able to reproduce most of the essential effects of polymers in

* Corresponding author. Tel.: +81-298-61-7257; fax: +81-298-61-7275.
E-mail address: kawaguchi.y@aist.go.jp (Y. Kawaguchi).

0142-727X/03/$ - see front matter © 2003 Elsevier Science Inc. All rights reserved.
doi:10.1016/S0142-727X(03)00059-6

Nomenclature

c	conformation tensor
f	friction factor
h	half height of the channel
p	pressure
Re_m	Reynolds number $= 2\rho u_m h/(\mu+\eta)$
Re_τ	Reynolds number $= \rho u_\tau h/(\mu+\eta)$
R_{uu}	two-point correlation coefficient
t	time
t^*	nondimensional time
u	velocity
u_m	mean velocity
u_τ	friction velocity
We_τ	Weissenberg number $= \rho\lambda u_\tau^2/(\mu+\eta)$
x	coordinate
x^*	nondimensional coordinate
Greeks	
α	mobility factor
β	ratio of solvent contribution to the total zero-shear viscosity $= \mu/(\mu+\eta)$.
η	dynamic viscosity of surfactant contribution
λ	relaxation time
μ	dynamic viscosity of solvent contribution
ρ	density
Superscripts and subscripts	
$(\ )^+$	normalized by wall units
$(\ )_{rms}$	root mean square fluctuations

dilute solution on the wall turbulence (Angelis et al., 2002). The role of elastic energy was studied in turbulence drag-reduction by polymer additives with an Oldroyd-B model (Min et al., 2001). Suzuki et al. first attempted to numerically study the drag-reducing flow with surfactant additives by using a Giesekus model (Suzuki et al., 2001), but they did not find any drag-reduction. The present study numerically examines the effect of Weissenberg number on flow structures for drag-reducing flow with surfactant additives.

2. Governing equations and boundary conditions

We simulate the fluid motion of the surfactant solution in a channel. The flow geometry and the coordinates are shown in Fig. 1, in which x, y and z are the streamwise, normal and spanwise direction respectively. The computational domain size is $L_x \times L_y \times L_z = 10h \times 2h \times 5h$. The measured rheological properties of the surfactant solution agree well with those of a Giesekus fluid (Suzuki et al., 2001; Kawaguchi et al., 2003). Thus a Giesekus model is used to describe the evolution of extra stress due to the deformation of macromolecules in the surfactant solution. The fluid is assumed to be incompressible and isothermal with constant properties. The governing equations for the surfactant solution can thus be written in dimensionless form as follows:

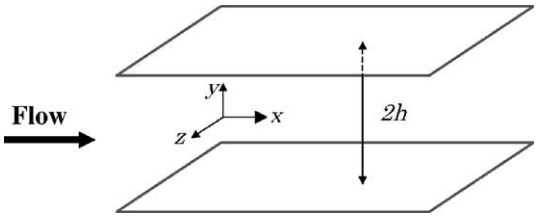

Fig. 1. Coordinate system in channel.

Continuity equation:

$$\frac{\partial u_i^+}{\partial x_i^+} = 0 \tag{1}$$

Momentum equation:

$$\frac{\partial u_i^+}{\partial t^*} + u_j^+ \frac{\partial u_i^+}{\partial x_j^*} = -\frac{\partial p^+}{\partial x_i^*} + \frac{\beta}{Re_\tau}\frac{\partial}{\partial x_j^*}\left(\frac{\partial u_i^+}{\partial x_j^*}\right) + \frac{1-\beta}{We_\tau} \times \frac{\partial c_{ij}^+}{\partial x_j^*} + \delta_{1i} \tag{2}$$

Constitutive equation:

$$c_{ij}^+ - \delta_{ij} + \alpha(c_{im}^+ - \delta_{im})(c_{mj}^+ - \delta_{mj}) + \frac{We_\tau}{Re_\tau}\left(\frac{\partial c_{ij}^+}{\partial t^*} + \frac{\partial u_m^+ c_{ij}^+}{\partial x_m^*} - \frac{\partial u_i^+}{\partial x_m^*}c_{mj}^+ - \frac{\partial u_j^+}{\partial x_m^*}c_{mi}^+\right) = 0 \tag{3}$$

In the above equations the following nondimensional variables are introduced:

$$x^* = \frac{x}{h}, \quad t^* = \frac{t}{h/u_\tau}, \quad u^+ = \frac{u}{u_\tau}, \quad p^+ = \frac{p}{\rho u_\tau^2},$$

$$c_{ij}^+ = c_{ij}, \quad Re_\tau = \frac{\rho u_\tau h}{\mu+\eta}, \quad We_\tau = \frac{\lambda\rho u_\tau^2}{\mu+\eta}$$

Conformation component c_{ij} is associated with the deformation of the long rod-like micelles and it has a simple relationship with the extra stresses τ_{ij} as $\tau_{ij} = \eta/\lambda(c_{ij} - \delta_{ij})$. The meanings of all the other variables are given in the Nomenclature. Note that the fluid motion is characterized by four parameters: Reynolds number, Weissenberg number, ratio β and mobility factor α. The larger the Weissenberg number, the

stronger the elasticity of the solution. In this study, we are interested in the effect of Weissenberg number on the flow structures. Thus we performed calculations for various Weissenberg numbers ($We_\tau = 2$, 12.5, 30 and 45), with other parameters fixed as $\alpha = 0.001$, $\beta = 0.9$ and $Re_\tau = 150$. The periodic boundary conditions are imposed in both the streamwise and spanwise direction, while the nonslip condition is adopted for the top and bottom walls.

3. Numerical procedure

A finite difference scheme is used to discretize the governing equations. A second-order central difference scheme is used for the spatial discretization except that MINMOD scheme is adopted for the discretization of the convective term in the constitutive equation. Numerical simulations of viscoelastic flow are prone to break down at high Weissenberg number due to the hyperbolic nature of the constitutive equations. To overcome this trouble, the artificial diffusion spectral method (Sureshkumar et al., 1997; Dimitropoulos et al., 1998) and local artificial diffusion finite difference scheme (Min et al., 2001) were employed. In a previous study, we compared the performance of the artificial diffusion scheme with a high-resolution scheme, MINMOD, for drag-reducing flow with additives in a channel (Yu and Kawaguchi, 2002), and found that the MINMOD scheme is much more stable and has higher spatial resolution than the artificial diffusion method. Therefore we used the MINMOD scheme in the present study. For time integration, the Adams–Bashforth scheme is used for all the terms except that the implicit method is used for the pressure term. The MAC method is employed to couple velocity and pressure.

A staggered grid system is used to prevent a checkboard pressure field. That is, velocity components are located at the cell interfaces while other variables are located at the nodes. Uniform grids are used in the streamwise and spanwise directions. Nonuniform grids are used in the normal direction with denser mesh near the wall to resolve small eddies. Fig. 2 compares the mean velocity profile and turbulence intensities by using two sets of grids: $64 \times 64 \times 64$ and $64 \times 128 \times 64$ grids (in the x-, y- and z-directions, respectively). It can be seen that the results for the two sets of grids agree well with each other. To save computational time, the $64 \times 64 \times 64$ grids are used in the present study. The grid spacings in the streamwise and spanwise directions are $\Delta x^+ = 23.4$ and $\Delta z^+ = 11.7$, respectively. Δy^+ varies from 0.45 next to the wall to about 9 near the center of the flow. The time-step used in the present computation is 0.001 h/u_τ.

4. Results and discussion

Fig. 3 compares the statistical steady-state values for $\alpha = 0.001$, $\beta = 0.9$, $Re_\tau = 150$ and four Weissenberg numbers $We_\tau = 2, 12.5, 30$ and 45. For comparison, the results of Newtonian fluid (set $\beta = 1.0$ in the momentum equation) are also presented. The streamwise mean velocity profiles are shown in Fig. 3(a). It is seen at $We_\tau = 2$, the nondimensionalized velocity profile is slightly smaller than that of the Newtonian case. This means that drag is not reduced but actually increased slightly. For $We_\tau =$ 12.5, 30 and 45, the velocity profiles are up-shifted at the buffer and logarithmic layers as compared to that of the Newtonian case. The larger flow rates mean that drag-reduction occurs. In this study, we define the drag-reduction rate as the percentage decrease of the friction factor as compared to Newtonian fluid flow at the same mean flow Reynolds number based on the height of the channel, $Re_\mathrm{m} = 2\rho u_\mathrm{m} h/(\mu + \eta) = 2Re_\tau u_\mathrm{m}^+$. The calculated mean Reynolds numbers and the corresponding friction factors are shown in Table 1. We did not perform the calculations for the Newtonian cases for those mean

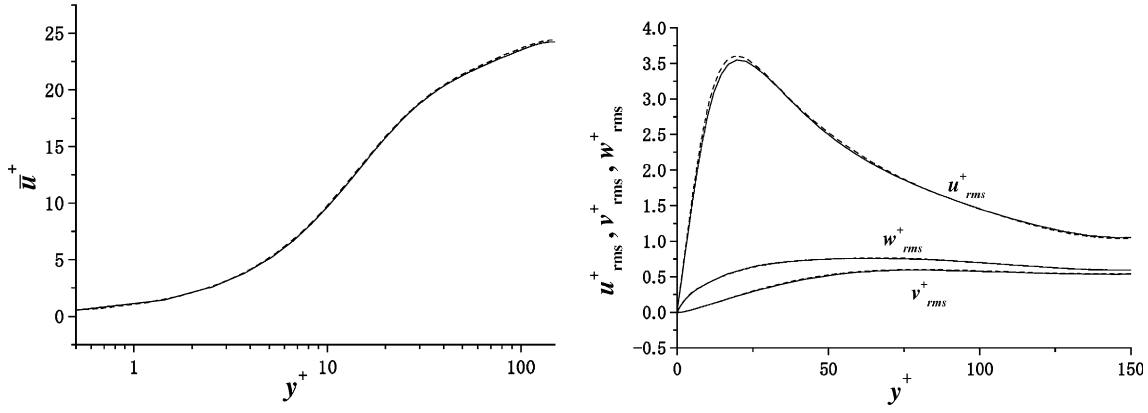

Fig. 2. (Left) The mean velocity profile and (right) root mean square velocity fluctuations for $\alpha = 0.001$, $\beta = 0.9$, $Re_\tau = 150$ and $We_\tau = 30$ and with two different grids: $64 \times 64 \times 64$ grids (solid line) and $64 \times 128 \times 64$ grids (dashed line).

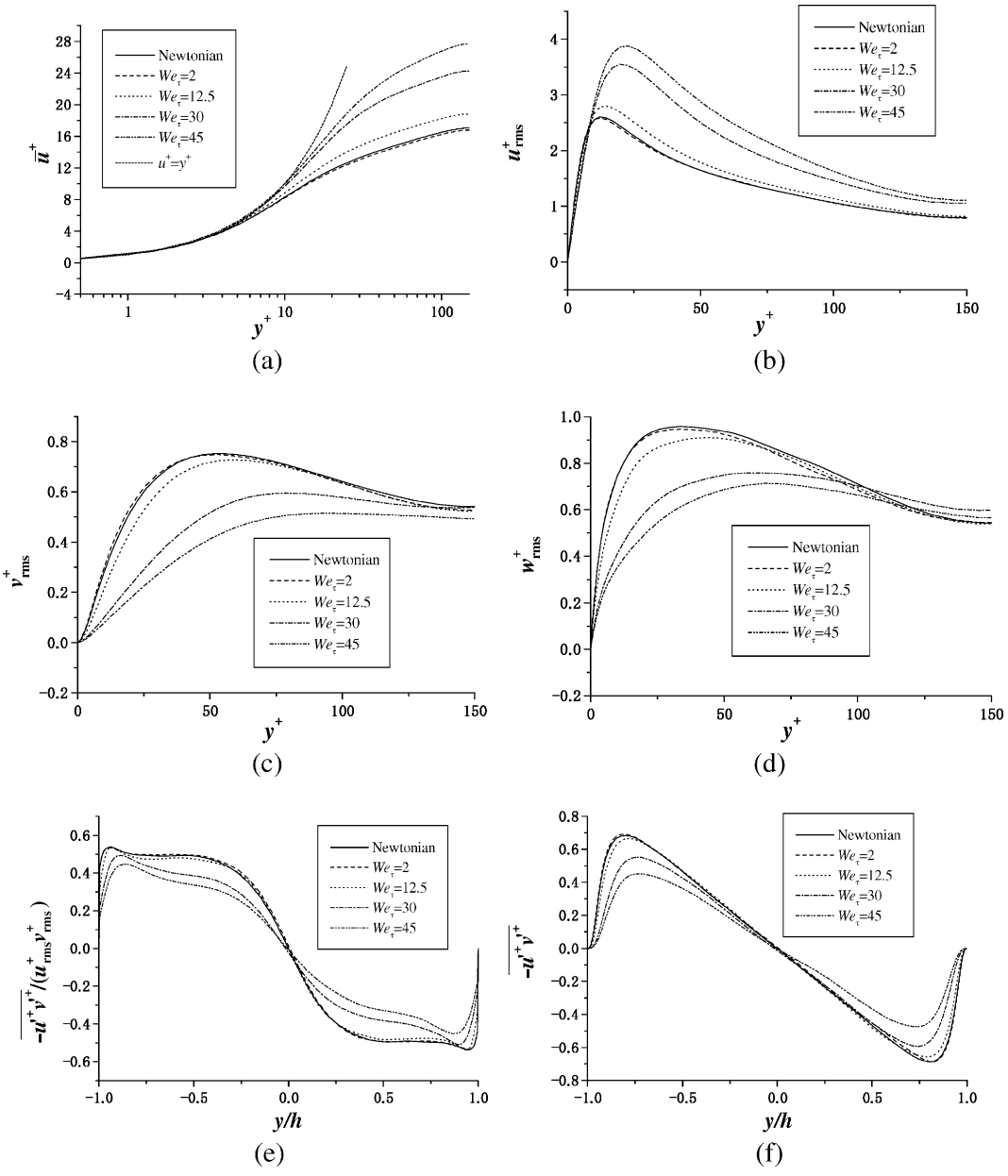

Fig. 3. Statistical steady-state values for Newtonian fluid at $Re_\tau = 150$ and surfactant solution at $\alpha = 0.001$, $\beta = 0.9$, $Re_\tau = 150$ and various Weissenberg numbers $We_\tau = 2$, 12.5, 30 and 45. (a) Mean velocity profile; (b)–(d) root mean velocity fluctuations; (e) correlation coefficient of u'^+ and v'^+; (f) Reynolds shear stress.

Table 1
Mean Reynolds numbers, friction factors and drag-reduction rate

Weissenberg number	12.5	30	45
Mean Reynolds number	4838	6180	6936
Friction factor	0.00769	0.00471	0.00374
Drag-reduction rate (%)	12.1	42.8	53.2

Reynolds numbers, but estimated the friction factors at those Reynolds numbers by using the experimental correlation $f = 0.073(Re_m)^{-0.25}$ (Dean, 1978), and obtained the drag-reduction rates listed in Table 1. Apparently the drag-reduction rate at $We_\tau = 12.5$ is appreciable. We performed the calculation for the case $We_\tau = 8$, and no appreciable drag-reduction was observed. Thus using the MINMOD scheme, the onset Weissenberg number obtained in the present study is around 10. Note that no appreciable drag-reduction is obtained at $We_\tau = 12.5$ by the artificial diffusion spectral method (Sureshkumar et al., 1997; Dimitropoulos et al., 1998). A higher onset Weissenberg number $12.5 < We_\tau < 25$ was predicted. This indicates that the artificial diffusion term reduces the accuracy of the solution. Moreover, it is clear from Fig. 3(a) that the larger the Weissenberg number, the larger the buffer layer becomes.

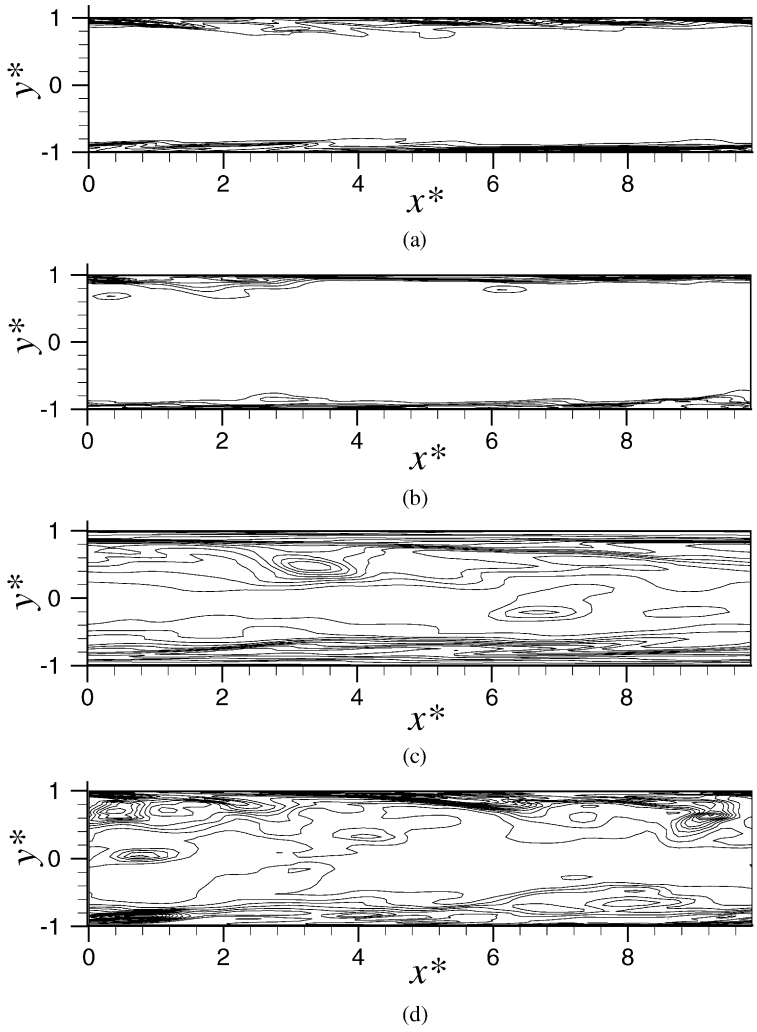

Fig. 4. Contours of instantaneous c_{xx}^{+} in the middle vertical x–y plane of the channel for the Giesekus fluid flow at $\alpha = 0.001$, $\beta = 0.9$, $Re_\tau = 150$ and four Weissenberg numbers: (a) $We_\tau = 2$; (b) $We_\tau = 12.5$; (c) $We_\tau = 30$ and (d) $We_\tau = 45$. Contour levels for $We_\tau = 2$, 12.5, 30 and 45 are 1.5–11, 37–545, 68–857 and 107–1520, respectively.

Fig. 3(b)–(d) compares the root mean square velocity fluctuations. It can be seen that for the smallest Weissenberg number $We_\tau = 2$, the turbulence intensities are almost the same as those of Newtonian results. As Weissenberg number increases, the root mean square velocity fluctuations in the streamwise direction are enhanced. The larger the Weissenberg number, the larger u_{rms}^{+} becomes. As compared to Newtonian results, the location of the maximum u_{rms}^{+} shifts toward the centerline of the channel for drag-reduction cases. The larger the drag-reduction rate, the further the location shifts to the bulk flow. This corresponds to an increased buffer layer with the increase of Weissenberg number. The root mean square velocity fluctuations in the normal direction decrease with the increase of Weissenberg number. On the whole, the root mean square velocity fluctuations in the spanwise direction also decrease with the increase of Weissenberg number except that at the center part of the channel, they are increased for the $We_\tau = 30$ and 45

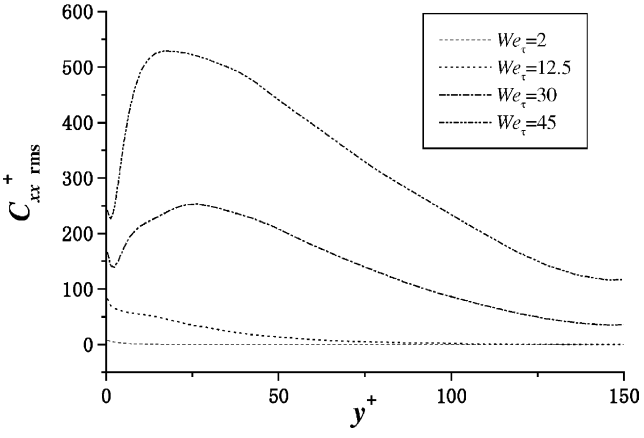

Fig. 5. Root mean square fluctuations for conformation component c_{xx}^{+} at $\alpha = 0.001$, $\beta = 0.9$, $Re_\tau = 150$ and four Weissenberg numbers $We_\tau = 2$, 12.5, 30 and 45.

cases. We can see that the appreciable enhancement of u^+_{rms} and the depression of v^+_{rms} and w^+_{rms} are located at the buffer layers, while in the corresponding logarithmic layers, the turbulent intensities do not change very much. This clearly shows that the surfactant additives primarily affect the phenomena occurring in the buffer layer.

Fig. 3(e) compares the velocity correlation coefficients for u and v. It is seen that as the Weissenberg number increases, the correlation coefficients decrease. The location of the maximum correlation coefficient shifts to the bulk flow as compared to the Newtonian case and nondrag-reduction case $We_\tau = 2$. Fig. 3(f) compares the Reynolds shear stress profiles. It is seen that the larger

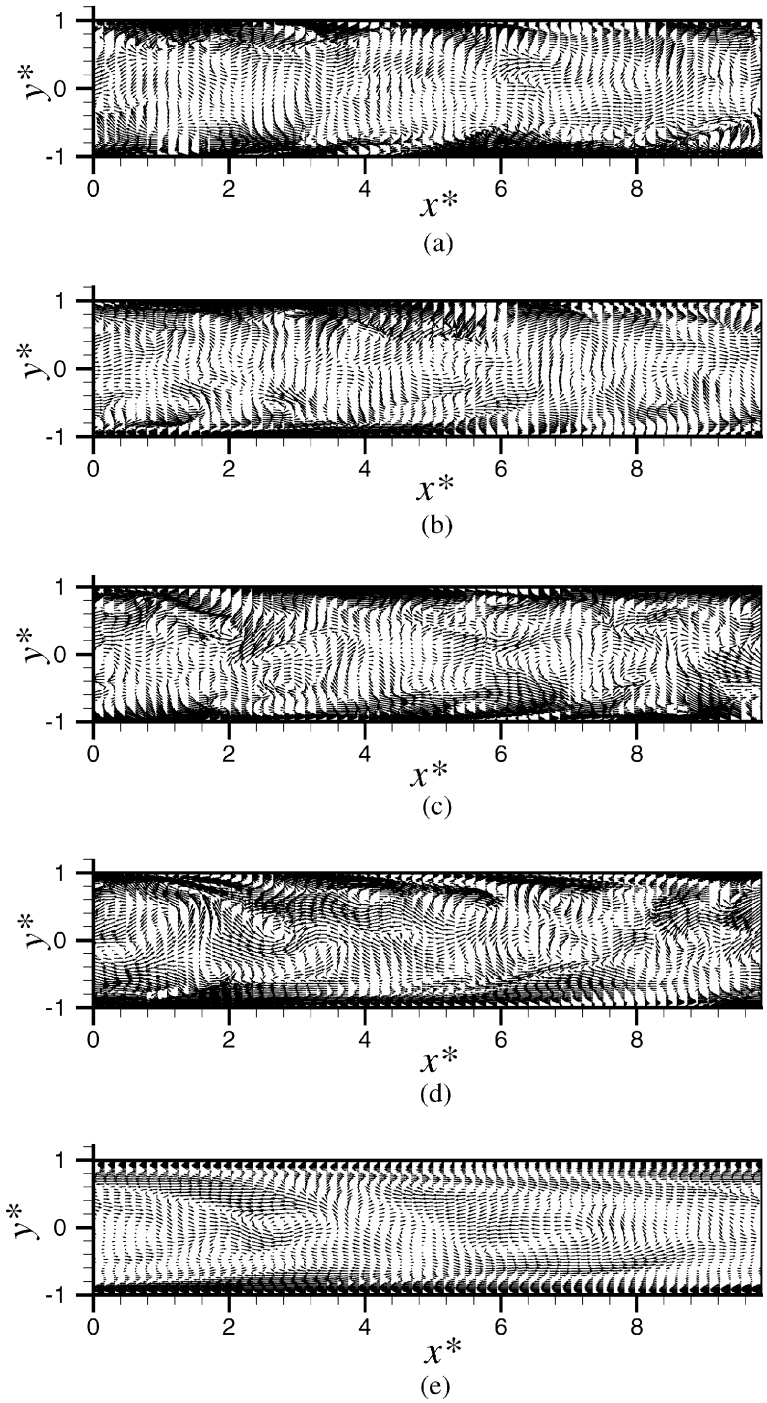

Fig. 6. Instantaneous velocity fluctuation field in the middle vertical x–y plane of the channel for (a) Newtonian fluid at $Re_\tau = 150$ and surfactant solution at $\alpha = 0.001$, $\beta = 0.9$, $Re_\tau = 150$ and four Weissenberg numbers: (b) $We_\tau = 2$; (c) $We_\tau = 12.5$; (d) $We_\tau = 30$ and (e) $We_\tau = 45$.

the drag-reduction rate, the smaller the Reynolds shear stress becomes. The location where the Reynolds shear stress reaches a maximum also shifts to the bulk flow for drag-reduction cases as compared to the Newtonian case.

Fig. 4 shows the instantaneous contour maps of the conformation component c_{xx}^{+} in the middle vertical x–y plane of the channel. It is seen that as the Weissenberg number increases, the value of c_{xx}^{+} increases greatly. The gradients near the wall become larger as the Weissenberg number increases. From this figure, we can partly explain why the calculation easily breaks down as the Weissenberg number increases. The steep conformation gradient is difficult to be captured accurately. Using high-order finite difference schemes or the spectral method, the steep gradients cannot be accurately captured and a negative eigen-value of the conformation tensor can be predicted. The unphysical values change the flow dynamics and usually result in breakdown of the solution. To prevent the numerical breakdown, artificial diffusion methods both for the spectral method and finite difference scheme were used by Sureshkumar et al. (1997), Dimitropoulos et al. (1998), and Min et al.

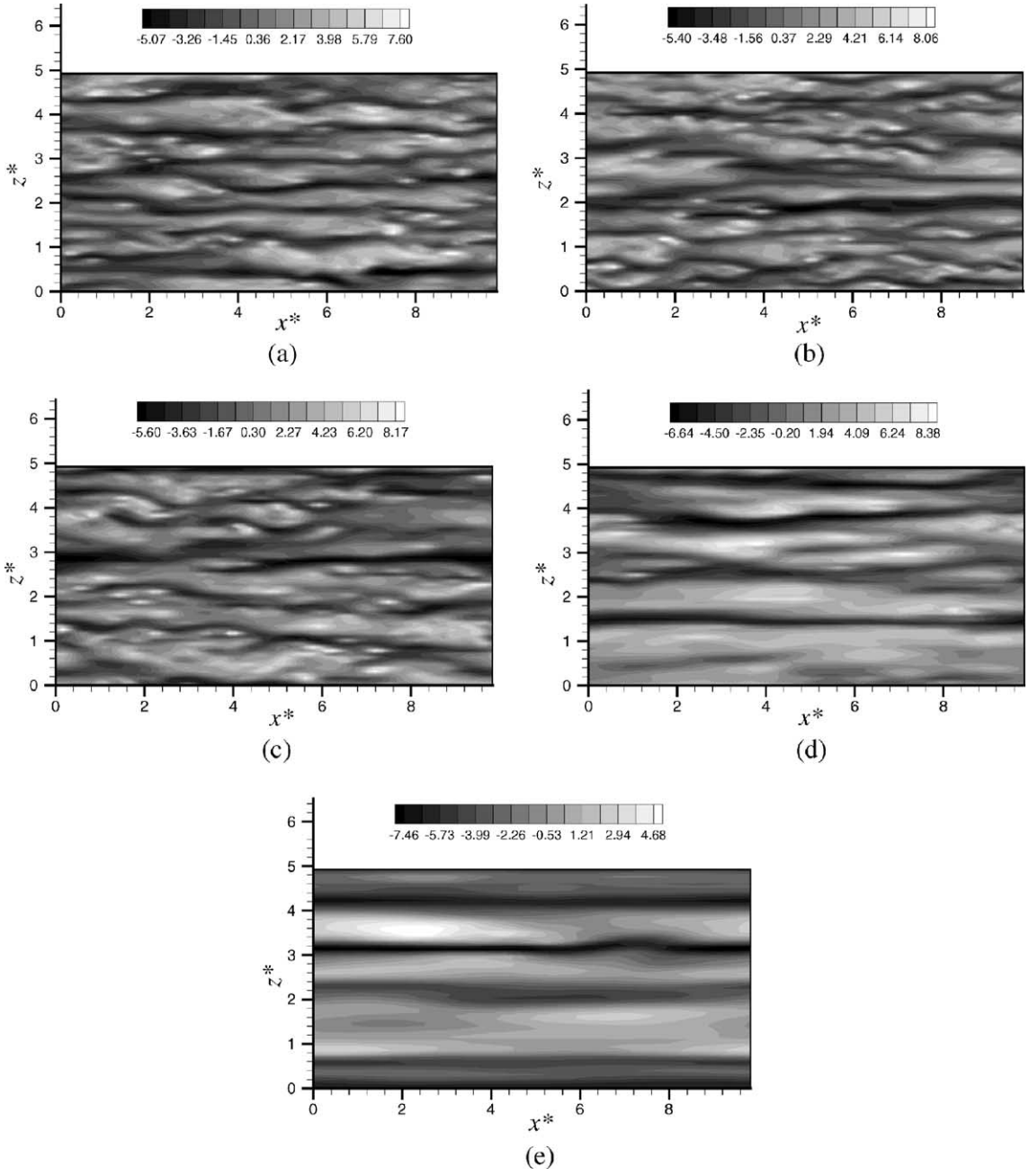

Fig. 7. Instantaneous snapshot of streamwise velocity fluctuation in the x–z plane at $y^{+} = 15$ for (a) Newtonian fluid at $Re_{\tau} = 150$ and surfactant solution at $\alpha = 0.001$, $\beta = 0.9$, $Re_{\tau} = 150$ and four Weissenberg numbers: (b) $We_{\tau} = 2$; (c) $We_{\tau} = 12.5$; (d) $We_{\tau} = 30$; (e) $We_{\tau} = 45$.

(2001), respectively. The calculation did not break down till $We_\tau = 50$ for the Giesekus fluid by using the artificial diffusion spectral method. However, too large artificial diffusion may greatly flatten the steep stress gradient (Yu and Kawaguchi, 2002) and the solution accuracy deteriorates. Therefore the high-resolution schemes such as MINMOD, which have been demonstrated to have a good capability to capture steep gradients, appear a good choice for the realistic simulation of turbulent viscoelastic flow.

Fig. 5 compares the root mean square of c_{xx}^+ fluctuations. It is seen that the conformation fluctuations become much stronger as the Weissenberg number increases. We believe that the strong fluctuations at high Weissenberg number may be another cause of the numerical instability and our calculation broke down in the cases of an even higher Weissenberg number, $We_\tau = 60$.

Fig. 6 shows instantaneous snapshots of the velocity fluctuation fields in the middle vertical x–y plane of the channel at different Weissenberg numbers (the streamwise velocity components are subtracted by a local mean velocity $u^+(y)$). For comparison, an instantaneous velocity field for the Newtonian case is also presented. It is clearly seen that the flow structure of the no drag-reduction case ($We_\tau = 2$) is similar to the Newtonian case. As the Weissenberg number increases the vortex structure becomes elongated in the streamwise direction, especially in the region near the walls. In Fig. 6(e), at the region near the bottom wall the fluid flows from right to left, which means that elongated low-speed streamwise streaks exist. To solve the larger flow structure, a larger computational domain may be required. The effect of computational domain size on the solutions is now being studied by our research group.

Fig. 7 shows instantaneous snapshots of the streamwise fluctuating velocity in the x–z plane at $y^+ = 15$. It is seen that as the Weissenberg number increases the low-speed streaks become more elongated and the average spacing of the streaks becomes wider. The larger spacing is connected with the larger flow structure such as that shown in Fig. 6. Fig. 8 shows the two-point correlations of streamwise velocity R_{uu} in the spanwise direction. The separation at which the minimum R_{uu} occurs can be used to estimate the mean spacing between high- and low-speed streaks, that is, the mean streak spacing is roughly twice the distance to the negative peak. It is seen more clearly from this picture that as the Weissenberg number increases the streak spacing becomes larger.

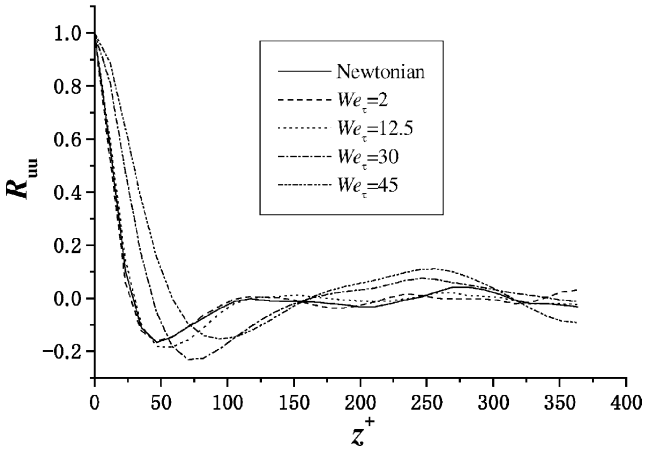

Fig. 8. Two-point spanwise correlation of the velocity component in the streamwise direction at $y^+ = 15$ for Newtonian fluid flow at $Re_\tau = 150$ and surfactant solution at $\alpha = 0.001$, $\beta = 0.9$, $Re_\tau = 150$ and four Weissenberg numbers $We_\tau = 2$, 12.5, 30 and 45.

5. Conclusion

The MINMOD scheme is used for the DNS study of surfactant solutions in a channel with a Giesekus model. We wished to investigate the effect of Weissenberg number on the flow structure, so in this study we changed the Weissenberg number We_τ from 2 to 45 with other parameters remaining fixed: $\alpha = 0.001$, $\beta = 0.9$ and $Re_\tau = 150$. From the numerical simulations, the following conclusions can be drawn. As the Weissenberg number increases the flow structures become larger. The larger the drag-reduction rate, the larger u_{rms}^+ increases and the smaller v_{rms}^+ and w_{rms}^+ decrease. The Reynolds shear stress becomes smaller as the Weissenberg number increases. As the Weissenberg number increases, both the streak spacing and the drag-reduction become larger. The onset Weissenberg number obtained in the present study was around 10, and the maximum drag-reduction obtained was 53%. We also partly explained why the calculations tend to break down in the case of high Weissenger number for viscoelastic flow simulation.

Acknowledgements

We are grateful to Prof. T. Kajishima at Osaka University, Dr. Y. Sato at National Institute of Advanced Industrial Science and Technology and Dr. K. Fukagata at Tokyo University for their valuable discussions on DNS. The first author also wants to give his cordial thanks to the colleagues: Dr. H. Yoshida, Dr. T. Matsunuma, Dr. Segawa, Dr. FC Li and Mrs. Hasegawa for their helps during this study. This study is supported by 'Ministry of Education, Culture, Sports, Science and Technology' through the project 'Smart Control of Turbulence: A Millennium Challenge for Innovative Thermal and Fluids System', Japan.

References

Angelis, E.De, Casciola, C.M., Piva, R., 2002. DNS of wall turbulence: dilute polymers and self-sustaining mechanisms. Comput. Fluids 31, 495–507.

Dean, R.B., 1978. Reynolds number dependence of ski friction and other bulk flow variables in two-dimensional rectangular duct flow. Trans. ASME, J. Fluids Eng. 100, 215–223.

DenToonder, J.M.J., Hulsen, M.A., Kuiken, G.D.C., Nieuwstadt, F.T.M., 1997. Drag reduction by polymer additives in a turbulent pipe flow: numerical and laboratory experiments. J. Fluid Mech. 337, 193–231.

Dimitropoulos, C.D., Sureshkumar, R., Beris, A.N., 1998. Direct numerical simulation of viscoelastic turbulent channel flow exhibiting drag reduction: effect of the variation of rheological parameters. J. Non-Newton. Fluid Mech. 79, 433–468.

Kawaguchi, Y., Wei, J.J., Yu, B., Feng, Z.P., 2003. Rheological characterization of drag-reducing cationic surfactant solution—shear and elongational viscosities of dilute solutions. In: Proceedings of the Fluids Engineering Division Summer Meeting, 1–10 July 2003, Honolulu, Hawaii.

Li, P.W., Kawaguchi, Y., Yabe, A., 2001. Transient heat transfer and turbulent characteristics of drag-reducing flow through a contracted channel. Enhanced Heat Transfer 8, 23–40.

Min, T., Yoo, J.Y., Choi, H., Joseph D.D., 2001. A role of elastic energy in turbulent drag reduction by polymer additives. In: Turbulence and Shear Flow Phenomena, Second International Symposium, KTH, Stockholm, vol. 3, pp. 35–50.

Orlandi, P., 1995. A tentative approach to the direct simulation of drag reduction by polymers. J. Non-Newton. Fluid Mech. 60, 277–301.

Sureshkumar, R., Beris, A.N., Handler, R.A., 1997. Direct numerical simulation of turbulent channel flow of a polymer solution. Phys. Fluids 9, 743–755.

Suzuki, H., Ishihara, K., Usui, H., 2001. Numerical study on a drag-reducing flow with surfactant additives. In: Proceedings 3rd Pacific Rim Conference on Rheology.

Toms, B.A., 1948. Some observation on the flow of linear polymer solutions through straight tubes at large Reynolds numbers. In: Proceedings of the 1st International Congress in Rheology, vol. 2. North Holland, Amsterdam, pp. 135–141.

Yu, B., Kawaguchi, Y., 2002. Numerical investigation on turbulent structures in a drag-reducing flow with surfactant additives in a 2D channel—comparison of artificial diffusion scheme and MINMOD scheme. In: Proceedings of the 5th JSME-KSME Fluids Engineering Conference, Nagoya, Japan.